

Tunable negative refraction without absorption in the optical regime

Jürgen Kästel and Michael Fleischhauer

Fachbereich Physik, Technische Universität Kaiserslautern, D-67663 Kaiserslautern, Germany

Susanne F. Yelin

Department Of Physics, University of Connecticut, Storrs, Connecticut 06269, USA and
ITAMP, Harvard-Smithsonian Center for Astrophysics, Cambridge, Massachusetts 02138, USA

Ronald L. Walsworth

Harvard-Smithsonian Center for Astrophysics and Department of Physics,
Harvard University, Cambridge, Massachusetts 02138, USA

(Dated: May 26, 2019)

PACS numbers:

Negative refraction of electromagnetic radiation [1] is currently one of the most active areas of photonics research, driven by goals such as the development of a “perfect lens” in which imaging resolution is not limited by electromagnetic wavelength [2]. Despite remarkable recent progress in demonstrating negative refraction using technologies such as meta-materials [3, 4, 5, 6] and photonic crystals [7, 8, 9], a key challenge remains the realization of negative refraction *without absorption* which is particularly important in the optical regime. Here we propose a promising new approach to this problem: the use of quantum interference effects similar to electromagnetically induced transparency (EIT) [10] to suppress absorption and induce chirality [11] in an ensemble of radiators (atoms, molecules, quantum dots, excitons, etc.). This technique allows negative refraction at densities where the magnetic susceptibility is still small and with refraction/absorption ratios that are orders of magnitude larger than those achievable previously. Furthermore, the value of the refractive index can be fine-tuned via external laser fields, which is essential for practical realization of sub-diffraction-limit imaging [12].

Early proposals for negative refraction required media with both negative permittivity and permeability ($\varepsilon, \mu < 0$) in the frequency range of interest. In the optical regime, however, it is difficult to realize negative permeability with low loss, since typical transition magnetic dipole moments (μ_a) are smaller than transition electric dipole moments (d_a) by a factor of the order of the fine structure constant $\alpha \sim \frac{1}{137}$. As a consequence the magnitude of magnetic susceptibilities χ_m are much smaller than that of electric susceptibilities χ_e :

$$|\chi_m| \sim \left(\frac{\mu_a}{d_a}\right)^2 |\chi_e| \sim \left(\frac{1}{137}\right)^2 |\chi_e|, \quad (1)$$

where $\varepsilon = 1 + \chi_e$ and $\mu = 1 + \chi_m$. Recently, Pendry sug-

gested an elegant way to alleviate this problem [13] by using a chiral medium, i.e., a medium in which the electric polarization \mathbf{P} is coupled to the free-space magnetic field component \mathbf{H} of an incident optical-frequency electromagnetic wave and the magnetization \mathbf{M} is coupled to the electric field component \mathbf{E} :

$$\begin{aligned} \mathbf{P} &= \varepsilon_0 \chi_e \mathbf{E} + \frac{\xi_{EH}}{c} \mathbf{H}, \\ \mathbf{M} &= \frac{\xi_{HE}}{c \mu_0} \mathbf{E} + \chi_m \mathbf{H}. \end{aligned} \quad (2)$$

Here ξ_{EH} and ξ_{HE} are the chirality coefficients, which in general can be complex. These terms lead to additional contributions to the refractive index [which in a non-chiral medium is just $n = \sqrt{\varepsilon \mu}$]:

$$n = \sqrt{\varepsilon \mu - \frac{(\xi_{EH} + \xi_{HE})^2}{4}} + \frac{i}{2}(\xi_{EH} - \xi_{HE}). \quad (3)$$

As Pendry noted, such a chiral medium allows $n < 0$ without requiring negative permeability if there is a positive imaginary part of $(\xi_{EH} - \xi_{HE})$ of sufficiently large magnitude. For example, choosing the phases of the complex chirality coefficients such that $\xi_{EH} = -\xi_{HE} = i\xi$, with $\xi, \varepsilon, \mu > 0$, the index of refraction becomes

$$n = \sqrt{\varepsilon \mu} - \xi, \quad (4)$$

and $n < 0$ when $\xi > \sqrt{\varepsilon \mu}$. Because chirality coefficients typically scale as $\xi_{EH}, \xi_{HE} \sim \frac{\mu_a}{d_a} \chi_e \sim \alpha \chi_e$ relative to the electric susceptibility, there is only one factor of α suppression as compared to $\chi_m \sim \alpha^2 \chi_e$. Nevertheless, the use of a chiral medium to achieve practical negative refraction in the optical regime still faces the demanding requirement of minimizing loss while realizing $|\xi_{EH}|, |\xi_{HE}| \sim 1$. In the following we describe how quantum interference effects similar to EIT allow this requirement to be met and also enable fine tuning of the refractive index by means of external laser fields.

To introduce concepts underlying electromagnetically-induced chiral negative refraction, we begin with the

simplistic three-level system shown in Fig. 1, which we will later modify to a more realistic scheme (see Fig. 2). As seen in Fig. 1, state $|1\rangle$ is coupled by an electric dipole transition to state $|3\rangle$ and by a magnetic dipole transition to state $|2\rangle$. The resonance frequency of the $|1\rangle - |2\rangle$ transition is nominally identical to that of the $|1\rangle - |3\rangle$ transition, such that the electric (**E**) and magnetic (**B**) components of the “probe field” (the electromagnetic wave that experiences negative refraction) can couple efficiently to the corresponding transitions. Furthermore, there is a strong resonant coherent field (the “coupling field”) that induces electric dipole transitions between states $|2\rangle$ and $|3\rangle$ with Rabi-frequency Ω_c . Since the $|2\rangle - |1\rangle$ transition is magnetic, level $|2\rangle$ can be considered meta-stable with a magnetic-dipole decay rate $\gamma_0 \sim (\mu_a/d_a)^2 \gamma \sim (1/137)^2 \gamma$, where γ is the corresponding electric-dipole decay rate out of level $|3\rangle$.

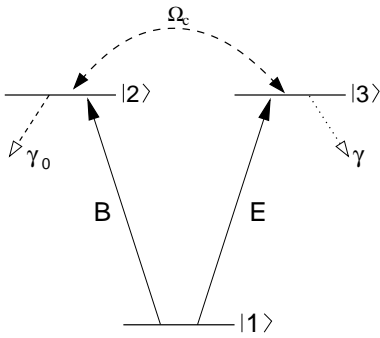


FIG. 1: A simplistic three-level system that allows concepts underlying electromagnetically-induced chiral negative refraction to be introduced. **E**, **B** are the electric and magnetic components of the probe field. γ_0 and γ are decay rates out of levels $|2\rangle$ and $|3\rangle$, respectively. Ω_c is an applied field that couples levels $|2\rangle$ and $|3\rangle$.

The scheme of Fig. 1 has similarities to schemes in resonant nonlinear optics based on EIT [14, 15]. For such schemes it is well known that there is destructive interference for the absorption and constructive interference for the dispersive cross-coupling between the $|1\rangle - |3\rangle$ and $|1\rangle - |2\rangle$ transitions in the limit $\gamma_0 \ll \gamma$ and if the transition $|1\rangle - |2\rangle$ is two-photon resonant with the probe field **E** and the coupling field Ω_c [10]. A similar set-up has been discussed recently by Oktel and Müstecaplioglu [16] for the purpose of generating negative refraction by means of a large negative permeability μ . However, they did not examine induced chirality and its effect on the index of refraction, which as we show below, is the most important contribution.

To enable electromagnetically-induced chiral negative refraction in realistic media, we modify the simplistic scheme of Fig. 1 to satisfy three criteria: (i) Ω_c must be an *ac* field, so that its phase can be adjusted to induce chirality; (ii) there must be high-contrast EIT for

the probe field; and (iii) the energy level structure must be appropriate for media of interest (atoms, molecules, excitons, etc.). In Fig. 2 we show one example of a modified energy level structure that meets the above criteria. This modified scheme employs strong coherent Raman coupling by two coherent fields with complex Rabi-frequencies Ω_1 and Ω_2 and carrier frequencies ω_1 and ω_2 , which creates a dark superposition of states $|1\rangle$ and $|4\rangle$. This dark state takes over the role of the ground state $|1\rangle$ in the three-level scheme of Fig. 1, such that the electric component of the probe field has a transition from the dark state to state $|3\rangle$ and the magnetic component a transition to level $|2\rangle$. Therefore, the modified scheme remains effectively three-level (consisting of $|2\rangle$, $|3\rangle$, and the dark state), but with sufficient additional degrees of freedom under experimental control to allow the above three criteria to be satisfied.

The coherent preparation of dark states by external laser fields is a well established technique realized in many systems. Existence of a dark state requires only two-photon resonance and is largely insensitive to the intensities of the laser fields. In the scheme of Fig. 2, coupling of the probe field to a dark state greatly enhances the freedom of choice of energy levels and operating conditions, and thus makes the scheme applicable to realistic systems. For example, the transition frequencies and selection rules can be chosen in such a way that the **E** and **B** components of the probe field couple predominantly to the transitions $|4\rangle - |3\rangle$ and $|1\rangle - |2\rangle$, respectively. The coupling between the two excited states $|2\rangle$ and $|3\rangle$ is now an *ac* coupling with carrier frequency ω_c and Rabi frequency Ω_c which can be chosen complex. By varying the phase of Ω_c the phase of ξ_{EH} and ξ_{HE} can be controlled. To ensure degeneracy between the electric and magnetic carrier frequencies, $\omega_1 - \omega_2 = \omega_c$ must hold. We note that the possibility of cross-coupling the electric and magnetic field components of a probe field without a common level coupled to both components was recently suggested by Thommen and Mandel [17] for meta-stable neon with a far-infrared probe field. However, their scheme exploits neither dark states nor chirality and thus the achieved ratio of negative refraction to absorption is small [18]. Finally, since the EIT transition in the level scheme of Fig. 2 is predominantly between levels $|4\rangle$ and $|2\rangle$, which can have comparable energies, the two-photon resonance can remain narrow even in the presence of one-photon-transition broadening mechanisms; and thus high-contrast EIT (i.e., minimal absorption of the probe field) is possible.

For an ensemble of radiators described by the level scheme of Fig. 2, we calculate the real and imaginary parts of the refractive index in the linear-response-limit. State $|2\rangle$ is assumed to be metastable since it couples to $|1\rangle$ only via a magnetic dipole transition, which as we show below allows absorption losses to be minimized. Similarly, state $|4\rangle$ is assumed to be stable. To model

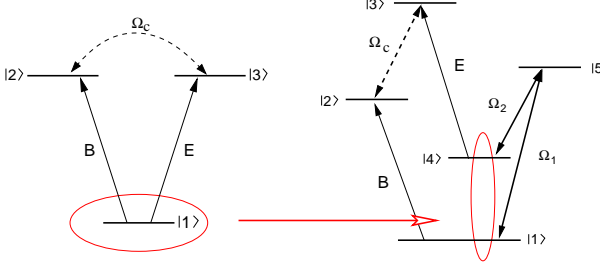


FIG. 2: Example of a modified level scheme to allow electromagnetically-induced chiral negative refraction in realistic media. The dark state created by the two-photon resonant Raman coupling of levels $|1\rangle$ and $|4\rangle$ takes over the role of level $|1\rangle$ in the simplistic three-level scheme of Fig.1. All coherent couplings Ω_c , Ω_1 , and Ω_2 can be optical or microwave dipole transitions.

realistic situations we take into account broadening of the intrinsically very narrow magnetic transition $|1\rangle - |2\rangle$ which could be due to relaxation other than radiative decay or due to inhomogeneous (e.g., Doppler) broadening. We also require that the $|2\rangle - |4\rangle$ transition, used for high-contrast EIT, has a very narrow linewidth. We solve for the steady-state values of the density matrix elements ρ_{34} and ρ_{21} , which determine the ensemble polarization $\mathbf{P} = Nd_{34}\rho_{34}$ and magnetization $\mathbf{M} = N\mu_{21}\rho_{21}$ respectively:

$$\rho_{34} = \alpha_{EE}\mathbf{E} + \alpha_{EH}\mathbf{B}, \quad \rho_{21} = \alpha_{HE}\mathbf{E} + \alpha_{HH}\mathbf{B}. \quad (5)$$

Here N is the density of radiators (atoms, molecules, excitons, etc.) and d_{34} and μ_{21} are the probe field transition electric and magnetic dipole moments. Explicit expressions for the polarizabilities (α_{EE} , α_{HH}) and chirality parameters (α_{EH} , α_{HE}) are given in the methods section. Fig. 3 shows typical calculated spectra for the electric and magnetic polarizabilities as well as the chirality parameters. The induced reduction of the electric polarizability α_{EE} and thus of the absorption on resonance is apparent. Likewise one recognizes a resonantly enhanced imaginary chirality α_{HE} while the other chirality α_{EH} and the magnetic polarizability α_{HH} remain very small.

Since we are interested in values for the refractive index substantially different from unity, we must take into account local field corrections. Due to the induced chirality, the probe magnetic field couples to the media by a factor $\simeq 137$ times stronger than in the case of non-chiral media. Therefore we include both electric and magnetic local field effects [19] to first order by replacing the macroscopic field values \mathbf{E} and \mathbf{B} in Eq. (5) with the local (i.e., microscopic) fields $\mathbf{E}_m = \mathbf{E} + \mathbf{P}/3\varepsilon_0$ and $\mathbf{B}_m/\mu_0 = \mathbf{H}_m = \mathbf{H} + \mathbf{M}/3$. (Higher-order corrections, e.g., modification of radiative decay rates, are not necessary for high-contrast EIT.) We then calculate the permittivity ε , permeability μ , and chirality coefficients ξ_{EH}

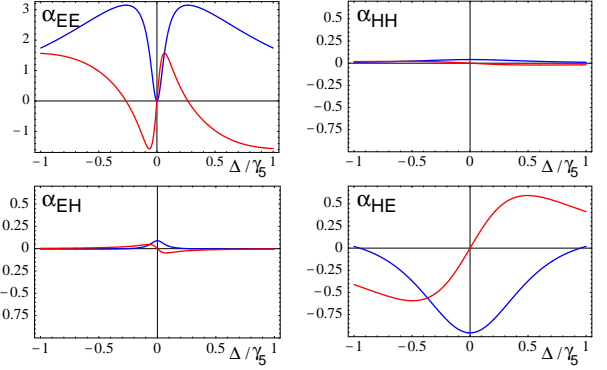


FIG. 3: Real (red) and imaginary (blue) parts of the electric (α_{EE}) and magnetic (α_{HH}) polarizabilities as well as the chirality parameters (α_{HE} , α_{EH}) in arbitrary but the same units, as a function of probe field detuning $\Delta = -\Delta_E = -\Delta_B$ relative to the radiative decay rate γ_3 from level $|3\rangle$. Here, $\Delta_E = \omega_{34} - \omega_{\text{probe}}$ and $\Delta_B = \omega_{21} - \omega_{\text{probe}}$, where ω_{probe} is the probe-field frequency and $\omega_{\mu\nu}$ is the transition frequency between levels $|\mu\rangle$ and $|\nu\rangle$. All coupling fields are resonant.

and ξ_{HE} with local field corrections, and determine the refractive index from Eq. (3). (For details see the methods section.)

As an example, Fig. 4(a) shows the calculated real and imaginary refractive index as a function of probe field detuning for a density of $N = 5 \cdot 10^{16} \text{ cm}^{-3}$ and using the realistic parameter values $\delta = 0$, $\Omega_1 = \Omega_2 = 10^6 \text{ s}^{-1}$, $\Omega_c = 10^4 e^{i\pi/2} \gamma_2$, $\gamma_2 = 10^3 \text{ s}^{-1}$, $\gamma_3 = \gamma_5 = (137)^2 \gamma_2$, $\gamma_4 \simeq 0$, and $\gamma_P = 10^4 \gamma_2$; and relating the transition dipole matrix elements to the radiative decay rates via $d_{34}(\mu_{21}/c) = \sqrt{\frac{3\pi\varepsilon_0\gamma_3(\gamma_2)\hbar c^3}{\omega^3}}$ for a typical optical wavelength of 600nm. (See the methods section for the definition of the above parameters; and note that the detunings and Rabi frequencies are given as angular frequencies.) We find substantial negative refraction and minimal absorption for this density, which is about a factor of 10^2 smaller than the density needed without taking chirality into account [16]. It should also be noted that the magnetic permeability differs by less than 10% from unity for the density considered here. Therefore, the negative refraction shown in Fig. 4(a) is clearly a consequence of chirality induced by quantum interference.

For larger N the optical response of the medium increases. For example, Fig. 4(b) shows the refractive index for $N = 5 \cdot 10^{17} \text{ cm}^{-3}$ with otherwise unchanged parameters. As expected the refraction (real part of n) reaches increasingly large negative values. Remarkably, we find that the absorption reaches a maximum and then decreases with increasing density. This effect is illustrated in Fig. 5 where we show the real and imaginary parts of the refractive index as well as the real part of μ (including local-field effects) as functions of the density. This peculiar behaviour is due to the term proportional to

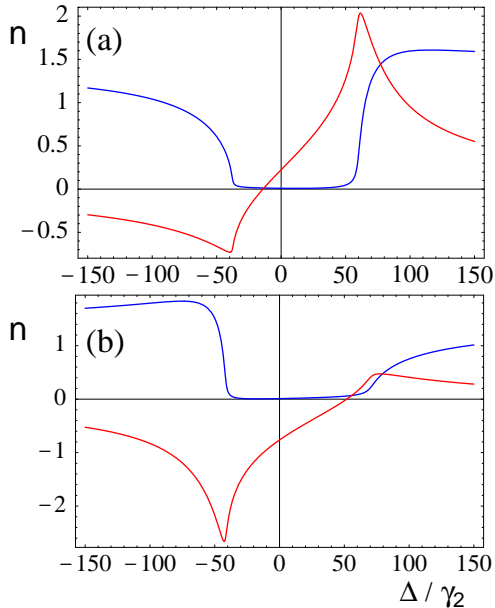


FIG. 4: Real (red) and imaginary (blue) parts of the refractive index, including local field effects, as a function of the probe field detuning $\Delta = -\Delta_E = -\Delta_B$ relative to the radiative decay rate γ_2 from level $|2\rangle$, for a density of (a) $N = 5 \cdot 10^{16} \text{ cm}^{-3}$ and (b) $N = 5 \cdot 10^{17} \text{ cm}^{-3}$. Other system parameters are given in the text and all coupling fields are resonant.

$(\xi_{EH} + \xi_{HE})^2$ in Eq. (3), which is nonzero in a broadened medium where $\xi_{EH} \neq -\xi_{HE}$ and can have a positive imaginary part and thus can partially compensate the imaginary part of $\epsilon\mu$. As a consequence the refraction/absorption ratio, shown in the inset of Fig. 5, continues to increase with density and reaches rather large values on the order of 10^2 . These results should be contrasted to previous theoretical proposals and experiments on negative refraction in the optical regime, for which the refraction/absorption ratio is typically on the order of unity.

It has been pointed out by Smith *et al.* and Merlin [12] that the realization of sub-diffraction-limit imaging with a lens of thickness d and resolution Δx requires an extreme fine tuning of the index of refraction to the value $n = -1$ with accuracy

$$\Delta n = \exp \left\{ -\frac{\Delta x}{2\pi d} \right\}. \quad (6)$$

The quantum interference scheme presented here provides a handle for such fine tuning. For example, as shown in Fig. 6, the real part of the refractive index can be fine tuned by relatively coarse adjustments of the strength of the coupling field Ω_c .

As with EIT and its applications — e.g., slow light and nonlinear optics [10] — electromagnetically-induced chiral negative refraction should be realizable in a wide

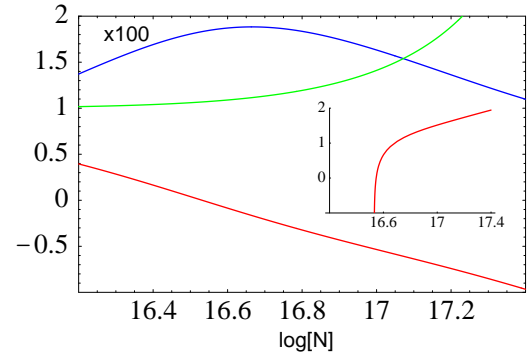


FIG. 5: Real (red) and imaginary (blue, $\times 100$) parts of the refractive index, as well as the real part of the permeability (green), as a function of the logarithm of the density N , at a frequency slightly below resonance ($\Delta = -25\gamma_2$) and including local field effects. Inset: $\log |Re(n)/Im(n)|$ as a function of $\log[N]$. Other system parameters are the same as for Fig. 4 and all coupling fields are resonant.

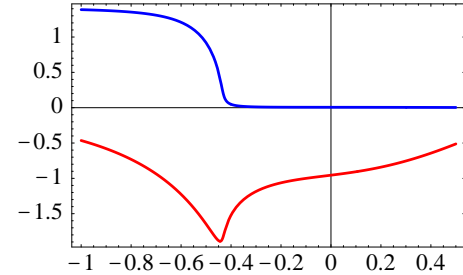


FIG. 6: Real (red) and imaginary (blue) parts of the refractive index as a function of the coupling field Rabi-frequency Ω_c relative to the radiative decay rate γ_3 , for $N = 3.5 \cdot 10^{17} \text{ cm}^{-3}$ and $\Delta = -\Delta_B = -\Delta_E = -25\gamma_2$. Other system parameters are the same as for Figs. 4 and 5 and all coupling fields are resonant.

range of atomic, molecular, and condensed matter systems. Already, a basic form of electromagnetically-induced chirality has been realized in Rb vapor [11]. In preparation for further experimental investigations we are currently performing a detailed assessment of systems such as metastable neon, rare-earths (dysprosium and others), as well as donor-bound electrons and bound excitons in semiconductors, all of which can have level structures and interactions analogous to those of the modified level scheme of Fig. 2. Results from these systems will be reported in future publications.

In conclusion, we combined Pendry's proposal for negative refraction in chiral media with concepts related to electromagnetically induced transparency (EIT). We found that EIT-like quantum interference can lead to a large induced chirality and simultaneously to a suppression of absorption under realistic conditions, thus enabling tunable negative refraction with

almost perfect cancellation of absorption. Like EIT, electromagnetically-induced chiral negative refraction should be applicable to a wide array of systems in the optical regime, including atoms, molecules, quantum dots, and excitons.

M.F. and J.K. thank the Institute for Atomic, Molecular and Optical Physics at the Harvard-Smithsonian Center for Astrophysics and the Harvard Physics Department for their hospitality and support. R.W. thanks D. Phillips for useful discussions. J.K. acknowledges financial support by the Deutsche Forschungsgemeinschaft through the GRK 792 “Nichtlineare Optik und Ultrakurzzeitphysik”. S.Y. thanks the Research Corporation for support.

[1] Veselago, V. G. The electrodynamics of substances with simultaneously negative values of ϵ and μ . *Sov. Phys. Usp.* **10**, 509 (1968).

[2] Pendry, J. B. Negative Refraction Makes a Perfect Lens. *Phys. Rev. Lett.* **85**, 3966 (2000).

[3] Pendry, J. B., Holden, A. J., Robbins, D. J. & Stewart, W. J. Magnetism from Conductors and Enhanced Non-linear Phenomena. *IEEE Trans. Micro. Theory Tech.* **47**, 2075 (1999).

[4] Smith, D. R., Padilla, W. J., Vier, D. C., Nemat-Nasser, S. C. & Schultz, S. Composite Medium with Simultaneously Negative Permeability and Permittivity. *Phys. Rev. Lett.* **84**, 4184 (2000); Shelby, R., Smith, D. R. & Schultz, S. Experimental Verification of a Negative Index of Refraction. *Science* **292**, 77 (2001).

[5] Yen, T. J. *et al.* Terahertz Magnetic Response from Artificial Materials. *Science* **303**, 1494 (2004).

[6] Linden, S. *et al.* Magnetic Response of Metamaterials at 100 Terahertz. *Science* **306**, 1351 (2004); Enkrich, C. *et al.* Magnetic Metamaterials at Telecommunication and Visible Frequencies. *Phys. Rev. Lett.* **95**, 203901 (2005).

[7] Parimi, P. V. *et al.* Negative Refraction and Left-Handed Electromagnetism in Microwave Photonic Crystals. *Phys. Rev. Lett.* **92**, 127401 (2004).

[8] Berrier, A. *et al.* Negative Refraction at Infrared Wavelengths in a Two-Dimensional Photonic Crystal. *Phys. Rev. Lett.* **93**, 073902 (2004).

[9] Lu, Z. *et al.* Three-Dimensional Subwavelength Imaging by a Photonic-Crystal Flat Lens Using Negative Refraction at Microwave Frequencies. *Phys. Rev. Lett.* **95**, 153901 (2005).

[10] Fleischhauer, M., Imamoglu, A. & Marangos, J. P. Electromagnetically induced transparency: Optics in coherent media. *Rev. Mod. Phys.* **77**, 633 (2005).

[11] Sautenkov, V. A. *et al.* Electromagnetically Induced Magnetochiral Anisotropy in a Resonant Medium. *Phys. Rev. Lett.* **94**, 233601 (2005).

[12] Smith, D. R. *et al.* Limitations on subdiffraction imaging with a negative refractive index slab. *Appl. Phys. Lett.* **82** 1506 (2003); Merlin, R. Analytical solution of the almost-perfect-lens problem. *Appl. Phys. Lett.* **84**, 1290 (2004).

[13] Pendry, J. B. A Chiral Route to Negative Refraction. *Science* **306**, 1353 (2004).

[14] Harris, S. E., Field, J. E. & Imamoglu, A. Nonlinear optical processes using electromagnetically induced transparency. *Phys. Rev. Lett.* **64**, 1107 (1990).

[15] Hakuta, K., Marmet, L. & Stoicheff, B. P. Electric-field-induced second-harmonic generation with reduced absorption in atomic hydrogen. *Phys. Rev. Lett.* **66**, 596 (1991).

[16] Oktel, M. Ö. & Müstecaplıoglu, Ö. E. Electromagnetically induced left-handedness in a dense gas of three-level atoms. *Phys. Rev. A* **70**, 053806 (2004).

[17] Thommen, Q. & Mandel, P. Electromagnetically Induced Left Handedness in Optically Excited Four-Level Atomic Media. *Phys. Rev. Lett.* **96**, 053601 (2006).

[18] In [17] a negative value for $\text{Im}[n]$ is given, corresponding to an amplifying medium; however this result is due to a calculational error, see Kästel, J. & Fleischhauer, M. quant-ph/0607150.

[19] Cook, D. M. *The Theory of the Electromagnetic Field*, Prentice-Hall (New Jersey).

METHODS

To determine the refractive index for the modified level scheme depicted in Fig. 2, we calculate the permittivity, permeability, and chirality coefficients for the Hamiltonian

$$H = \sum_{n=1}^5 \hbar \omega_n^A |n\rangle \langle n| + \left\{ -\frac{1}{2} d_{34} E e^{-i\omega_p t} |3\rangle \langle 4| - \frac{1}{2} \mu_{21} B e^{-i\omega_p t} |2\rangle \langle 1| - \frac{\hbar}{2} \Omega_1 e^{-i\omega_1 t} |5\rangle \langle 1| - \frac{\hbar}{2} \Omega_2 e^{-i\omega_2 t} |5\rangle \langle 4| - \frac{\hbar}{2} \Omega_c e^{-i\omega_c t} |3\rangle \langle 2| + \text{H.c.} \right\}; \quad (\text{M.1})$$

which, together with

$$\Gamma = \sum_{n=2}^5 \gamma_n |n\rangle \langle n| \quad (\text{M.2})$$

describing the radiative decay with rates γ_n out of level $|n\rangle$, leads to the density matrix equation

$$\dot{\rho} = -\frac{i}{\hbar} [H, \rho] - \frac{1}{2} [\Gamma, \rho]_+. \quad (\text{M.3})$$

In order to solve for the steady-state values of the density matrix elements ρ_{34} and ρ_{21} in a linear response approximation, we treat \mathbf{E} and \mathbf{B} as small variables. In zeroth order of these fields we therefore solve the equations for the subsystem $\{|1\rangle, |4\rangle, |5\rangle\}$ exactly since the couplings Ω_1 and Ω_2 are strong. Under the condition $\gamma_4 = 0$ this leads to

$$\begin{aligned} \rho_{11}^{(0)} &= \frac{\Omega_2^2}{\Omega_1^2 + \Omega_2^2} & \rho_{44}^{(0)} &= \frac{\Omega_1^2}{\Omega_1^2 + \Omega_2^2} \\ \rho_{41}^{(0)} &= -\frac{\Omega_1 \Omega_2}{\Omega_1^2 + \Omega_2^2} & \rho_{55}^{(0)} &= \rho_{51}^{(0)} = \rho_{45}^{(0)} = 0, \end{aligned} \quad (\text{M.4})$$

which gives the well known dark state $|D\rangle = \frac{1}{\sqrt{\Omega_1^2 + \Omega_2^2}} (\Omega_2 |1\rangle - \Omega_1 |4\rangle)$. To proceed we plug this into the equations for the remaining density matrix elements

(in the rotating frame):

$$\begin{aligned} \dot{\rho}_{21} &= - (i\Delta_B + \gamma_{21}) \rho_{21} + \frac{i}{2} \left\{ \frac{\mu_{21} B}{\hbar} \rho_{11}^{(0)} + \Omega_c^* \rho_{31} \right\} \\ \dot{\rho}_{31} &= - (i(\Delta_B + \delta) + \gamma_{31}) \rho_{31} + \frac{i}{2} \left\{ \frac{d_{34} E}{\hbar} \rho_{41}^{(0)} - \frac{\mu_{21} B}{\hbar} \rho_{32} + \Omega_c \rho_{21} \right\} \\ \dot{\rho}_{43} &= - (-i\Delta_E + \gamma_{34}) \rho_{43} + \frac{i}{2} \left\{ -\frac{d_{34} E}{\hbar} \rho_{44}^{(0)} - \Omega_c^* \rho_{42} \right\} \\ \dot{\rho}_{42} &= - (i(-\Delta_E + \delta) + \gamma_{42}) \rho_{42} + \frac{i}{2} \left\{ \frac{d_{34} E}{\hbar} \rho_{32} - \frac{\mu_{21} B}{\hbar} \rho_{41}^{(0)} - \Omega_c \rho_{43} \right\} \\ \dot{\rho}_{32} &= - (i\delta + \gamma_{32}) \rho_{32} + \frac{i}{2} \left\{ \frac{d_{34} E}{\hbar} \rho_{42} - \frac{\mu_{21} B}{\hbar} \rho_{31} \right\} \end{aligned} \quad (\text{M.5})$$

The off-diagonal decay rates γ_{ij} are given by $2\gamma_{ij} = \gamma_i + \gamma_j$ and the detunings are defined as $\Delta_E = \omega_{34} - \omega_{\text{probe}}$, $\Delta_B = \omega_{21} - \omega_{\text{probe}}$, and $\delta = \omega_{52} - \omega_c$, with $\omega_{\mu\nu}$ being the transition frequencies between levels $|\mu\rangle$ and $|\nu\rangle$. The stationary solutions for the relevant matrix elements ρ_{34} and ρ_{21} in linear response read:

$$\begin{aligned} \rho_{34}^{(1)} &= \alpha_{EE} \mathbf{E} + \alpha_{EH} \mathbf{B} \\ \rho_{21}^{(1)} &= \alpha_{HE} \mathbf{E} + \alpha_{HH} \mathbf{B} \end{aligned} \quad (\text{M.6})$$

with the diagonal polarizabilities

$$\begin{aligned} \alpha_{EE} &= \frac{id_{34}}{2\hbar} \frac{\rho_{44}^{(0)} (\gamma_{42} + i(\Delta_E - \delta))}{(\gamma_{42} + i(\Delta_E - \delta))(\gamma_{34} + i\Delta_E) + |\Omega_c|^2/4} \\ \alpha_{HH} &= \frac{i\mu_{21}}{2\hbar} \frac{\rho_{11}^{(0)} (\gamma_{31} + i(\Delta_B + \delta))}{(\gamma_{21} + i\Delta_B)(\gamma_{31} + i(\Delta_B + \delta)) + |\Omega_c|^2/4} \end{aligned} \quad (\text{M.7})$$

and the off-diagonal chirality parameters

$$\begin{aligned} \alpha_{EH} &= - \frac{\mu_{21}}{4\hbar} \frac{\rho_{41}^{(0)} \Omega_c}{(\gamma_{42} + i(\Delta_E - \delta))(\gamma_{34} + i\Delta_E) + |\Omega_c|^2/4} \\ \alpha_{HE} &= - \frac{d_{34}}{4\hbar} \frac{\rho_{41}^{(0)} \Omega_c^*}{(\gamma_{21} + i\Delta_B)(\gamma_{31} + i(\Delta_B + \delta)) + |\Omega_c|^2/4}. \end{aligned} \quad (\text{M.8})$$

To account for non-radiative broadening we add an additional dephasing rate γ_P to the decay rates γ_{ij} , $i \neq j$. Note, that levels $|2\rangle$ and $|4\rangle$ are assumed to have approximately the same energy such that they experience the same phase fluctuations; hence γ_{42} , which is relevant for EIT, remains essentially unbroadened. In contrast, due to the large energy difference of the involved states, γ_{21} and γ_{34} encounter a broadening γ_P , likewise γ_{31} experiences a broadening $2\gamma_P$. For our particular system a

non-radiative broadening is incorporated by modifying the rates γ_{ij} in (M.7,M.8) in the following way:

$$\begin{aligned}\gamma_{42} &\longrightarrow \gamma_{42} \\ \gamma_{21} &\longrightarrow \gamma_{21} + \gamma_P \\ \gamma_{34} &\longrightarrow \gamma_{34} + \gamma_P \\ \gamma_{31} &\longrightarrow \gamma_{31} + 2\gamma_P\end{aligned}\tag{M.9}$$

Expressing the permittivity ε , permeability μ , and chirality coefficients ξ_{EH} and ξ_{HE} in terms of the polarizabilities and chiralities α , and taking into account local-field corrections as described in the main text, yields

$$\begin{aligned}\xi_{EH} &= \sqrt{\frac{\mu_0}{\varepsilon_0} \frac{Nd_{34}}{\mathcal{L}^{\text{loc}}}} \alpha_{EH}, \\ \xi_{HE} &= \sqrt{\frac{\mu_0}{\varepsilon_0} \frac{N\mu_{21}}{\mathcal{L}^{\text{loc}}}} \alpha_{HE},\end{aligned}\tag{M.10}$$

$$\begin{aligned}\varepsilon &= 1 + \frac{Nd_{34}}{\varepsilon_0 \mathcal{L}^{\text{loc}}} \times \\ &\quad \left\{ \alpha_{EE} + \frac{N}{3} \mu_0 \mu_{21} \left(\alpha_{EH} \alpha_{HE} - \alpha_{EE} \alpha_{HH} \right) \right\}, \\ \mu &= 1 + \frac{N\mu_{21}}{\mathcal{L}^{\text{loc}}} \times \\ &\quad \left\{ \alpha_{HH} + \frac{N}{3} \frac{d_{34}}{\varepsilon_0} \left(\alpha_{EH} \alpha_{HE} - \alpha_{EE} \alpha_{HH} \right) \right\},\end{aligned}\tag{M.11}$$

$$\begin{aligned}\mathcal{L}^{\text{loc}} &= 1 - \frac{N}{3} \frac{d_{34}}{\varepsilon_0} \alpha_{EE} - \frac{N}{3} \mu_0 \mu_{21} \alpha_{HH} \\ &\quad - \left(\frac{N}{3} \right)^2 \frac{d_{34}}{\varepsilon_0} \mu_0 \mu_{21} \left(\alpha_{EH} \alpha_{HE} - \alpha_{EE} \alpha_{HH} \right).\end{aligned}\tag{M.12}$$

Note that here $\xi_{EH} \neq -\xi_{HE}$ since $\gamma_{42} \neq \gamma_{21}$ and $\gamma_{34} \neq \gamma_{31}$.